Research Article | Vol. 26, No. 7 | 2 Apr 2018 | OPTICS EXPRESS 8679
Optics EXPRESS

Optimum power allocation for uniform illuminance in indoor visible light communication

G. V. S. S. Praneeth Varma*

Department of Electrical Engineering, Indian Institute of Technology Hyderabad, Telangana, 502285, India
ee14resch11007@iith.ac.in

Abstract: In this paper an optimal power allocation scheme is proposed to acheive uniform illuminance. Regular arrays and random geometries are considered for an arrangement of the source LEDs. Uniform illuminance is accomplished by considering the variance of the received power on the receiver plane as metric and framing it as a convex optimization problem. Numerical results show that the quality factor of random geometries are superior to fixed geometries. While preserving uniformity, the cost of the system can be reduced when random geometries are used.

OCIS codes: (260.0260) Physical optics; (230.3670) Light-emitting diodes.

References and links

1. H. Guo-yong, C. Chang-ying, and C. Zhen-qiang, "Free-space optical communication using visible light," J. Zhejiang Univ. Sci. A **8**(2), 186–191 (2007).
2. J. Kovác, J. Jakabovic, and M. Kytka, "Advanced light emitting devices for optoelectronic applications," Proc. SPIE **7138**, 71382A1 (2008).
3. J. Kahn and J. Barry, "Wireless infrared communications," Proc. IEEE **85**(2), 265–298 (1997).
4. T. Komine and M. Nakagawa, "Fundamental analysis for visible-light communication system using led lights," IEEE Trans. Consum. Electron. **50**(1), 100–107 (2004).
5. A. Anusree and R. K. Jeyachitra, "Performance analysis of a MIMO vlc (visible light communication) using different equalizers," in *Proceedings of International Conference on Wireless Communications Signal Processing and Networking* (IEEE, 2016), pp. 43–46.
6. R. Bai, R. Jang, J. Tan, and J. Quan, "Performance comparison of vlc MIMO techniques considering indoor illuminance with inclined LEDs," in P*roceedings of International Conference on Wireless for Space and Extreme Environments* (IEEE, 2016), pp. 105–110.
7. P. F. Mmbaga, J. Thompson, and H. Haas, "Performance analysis of indoor diffuse vlc MIMO channels using angular diversity detectors," J. Lightwave Technol. **34**(4), 1254–1266 (2016).
8. A. Burton, H. L. Minh, Z. Ghassemlooy, S. Rajbhandari, and P. A. Haigh, "Performance analysis for 180° receiver in visible light communications," in *Proceedings of International Conference on Communications and Electronics* (IEEE, 2012), pp. 48–53.
9. L. Zeng, D. O'Brien, H. Le-Minh, K. Lee, D. Jung, and Y. Oh, "Improvement of date rate by using equalization in an indoor visible light communication system," in *Proceedings of International Conference on Circuits and Systems for Communications* (IEEE, 2008), pp. 678–682.
10. Y. Chen, C. W. Sung, S.-W. Ho, and W. S. Wong, "Ber analysis for interfering visible light communication systems," in *Proceedings of International Symposium on Communication Systems Networks and Digital Signal Processing* (IEEE, 2016), pp. 1–6.
11. Q. Wang, Z. Wang, and L. Dai, "Multiuser MIMO-OFDM for visible light communications," IEEE Photonics J. **7**(6), 1–11 (2015).
12. T. Fath and H. Haas, "Performance comparison of mimo techniques for optical wireless communications in indoor environments," IEEE Trans. Commun. **61**(2), 733–742 (2013).
13. Z. Wang, C. Yu, W.-D. Zhong, J. Chen, and W. Chen, "Performance of a novel led lamp arrangement to reduce snr fluctuation for multi-user visible light communication systems," Opt. Express **20**(4), 4564–4573 (2012).
14. N. Wittels and M. A. Gennert, "Optimal lighting design to maximize illumination uniformity," Proc. SPIE **2348**, 46–56 (1994).
15. M. A. Gennert, N. Wittels, and G. L. Leatherman, "Uniform frontal illumination of planar surfaces: where to place the lamps," Opt. Eng. **32**(6), 1261–1271 (1993).
16. I. Moreno, "Design of led spherical lamps for uniform far-field illumination," Proc. SPIE **6046**, 60462E (2016) .
17. I. Moreno, M. Avendaño-Alejo, and R. I. Tzonchev, "Designing light-emitting diode arrays for uniform near-field irradiance," Appl. Opt. **45**(10), 2265–2272 (2006).

#320991 https://doi.org/10.1364/OE.26.008679
Journal © 2018 Received 30 Jan 2018; revised 15 Mar 2018; accepted 15 Mar 2018; published 26 Mar 2018

Optics EXPRESS

18. P. Lei, Q. Wang, and H. Zou, "Designing LED array for uniform illumination based on local search algorithm," J. Europ. Opt. Soc. Rap. Public. **9**, 140141 (2014).
19. J. Ding, Z. Huang, and Y. Ji, "Evolutionary algorithm based power coverage optimization for visible light communications," IEEE Commun. Lett. **16**(4), 439–441 (2012).
20. Y. Liu, Y. Peng, Y. Liu, and K. Long, "Optimization of receiving power distribution using genetic algorithm for visible light communication," Proc. SPIE **9679**, 96790I (2015).
21. Sourav Pal, "Optimization of LED array for uniform illumination over a target plane by evolutionary programming," Appl. Opt. **54**(27), 8221–8227 (2015).
22. G.V.S.S.Praneeth Varma, Rayapati Sushma, Vandana Sharma, Abhinav Kumar, and G.V.V.Sharma, "Power allocation for uniform illumination with stochastic LED arrays," Opt. Express **25**(8), 8659–8669 (2017).
23. M. Haenggi, "Mean interference in hard-core wireless networks," IEEE Commun. Lett. **15**(8), 792–794 (2011).
24. J. Grubor, O. C. G. Jamett, J. W. Walewski, and K. d. Langer, "High-speed wireless indoor communication via visible light," in *ITG Fachbericht* (2007), pp. 203-208.
25. S.Boyd and L.Vandenberghe, *Convex Optimization*, (Cambridge University, 2004).

1. Introduction

In recent years, there has been immense interest in visible light communication (VLC), because of the benefits it provides in terms of security and high data rates, conserving radio frequency (RF) spectrum as well as power. Traditional light sources have been replaced by cost-effective light-emitting diodes (LEDs) for their longevity, lower power consumption, fast switching times etc.. This resulted in using LEDs as light sources for digital communication [1–4]. Significant amount of research has been done in adapting well known wireless techniques to indoor VLC [5–12].

Fair amount of existing literature has focused on implementing wireless technologies like multiple-input and multiple-output(MIMO), orthognal frequency division multiplexing (OFDM), and equalization techniques in VLC. The performance of MIMO VLC is analyzed for different equalizers in [5]. An LED inclined MIMO (LIM) model is proposed and compared with an LED vertical MIMO (LVM) in [6]. In [7], the angular diversity is obtained by placing multiple photodetectors on a receiver node with a curved surface. A similiar receiver is discussed in [8]. Equalization is employed at the receiver to improve the data rate in [9]. In [10], an expression for the BER in the presence of interference is obtained. However, the primary objective of any light source is to provide uniform illuminance, which was usually not taken into account in [5–10]. Uniformity is useful in communication scenario, since it ensures uniform signal strength across the room and results in better coverage [13].

One approach in realizing uniform illuminance is the arrangement of the source LEDs. In [14, 15], uniform illumination is obtained by finding higher order partial derivatives of the received power at a point close to origin and equating to zero. This ensures uniformity only in the neighbourhood of origin. Similar approach is used in [16, 17] to obtain optimum spacing between LEDs in square array and optimum radii in case of circular arrays. Local search algorithm is employed in [18] to find the optimum location of the LEDs. The solution is obtained by iterative process and remains sub-optimal if the time bound is elapsed. Evolutionary algorithms are proposed in [19–21] to obtain uniform illuminance on the receiver plane. However, adverse configurations in the algorithm may lead to local extremum and not the global extremum. In all the above, computationally intensive optimization routines were used for optimum location of the LED sources to realise uniform illuminance on the incident surface.

Uniform illuminance can also be obtained by appropriate allocation of power to an arrangement of the source LEDs. A trial and error approach for power allocation for uniform illuminance is used in [13] for a combination of circular square geometry in order to illuminate the edges of the incident surface. In [22], the light sources are modeled using stochastic geometry by locating them randomly in an indoor environment, generating average uniform illumination with appropriate power allocation.

Some of the above literature has focused on a regular geometry with equal power allocation to individual LED sources. While a binomial point process (BPP) based stochastic model is

Optics EXPRESS

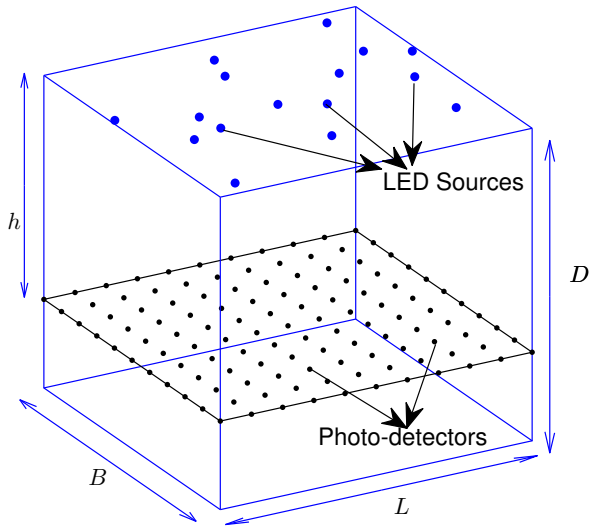

Fig. 1. System model.

a powerful tool for resource allocation for VLC [22], it is useful to consider power allocation for a VLC based on a single realization of a stochastic point process. Here, a Matern type II hard-core point process (HCPP) is desirable and more appropriate, since it accounts for minimum separation between any two LEDs for better coverage and reduced interference between adjacent LEDs. The problem of finding optimal power allocation for a realization of HCPP is addressed in this paper. This is done by considering the variance of the power on the receiver plane as an objective function. This function is shown to be convex, allowing for optimum power allocation. Through numerical results, it is shown that this approach is superior to existing techniques for power allocation and also reduces the cost of the system in terms of the number of LEDs.

2. System model

Let P_{t_i} is the transmit power at the ith LED in Fig. 1. The received power at photo-detector j is given by

$$P_{r_j} = \sum_{i=1}^{N} H_{ij} P_{t_i}, \tag{1}$$

where H_{ij} is the channel gain between the transmiter LED i and the photo-detector j. All the above parameters are well defined and are available in [13, 22]. The analysis is carried out for the geometries listed in Table. 1. All the LEDs are located vertical to the plane where the photo-detector is placed as shown in Fig. 1.

Optics EXPRESS

Table 1. **Arrangement of LEDs in Different Geometries**

Geometry	LED arrangement	Remarks
Square	$a_n, b_n \in S$	$S = \{\frac{\sqrt{N}+1-2(i+1))d}{2}\}$ and $d = \frac{L}{\sqrt{N}}$, $\forall i = \{1, \cdots, \sqrt{N}\}$.
Circle-square	$a_n = \begin{cases} r\cos(\theta_n) & n \le N-4 \\ (-1)^{\lfloor \frac{n-1}{2} \rfloor} z & N-3 \le n \le N \end{cases}$ $b_n = \begin{cases} r\sin(\theta_n) & 1 < n \le N-4 \\ (-1)^n z & N-3 \le n \le N \end{cases}$	$r = 2.2, z = 2.4,$ $\theta_n = \begin{cases} \frac{2\pi(n-1)}{N-4} & 1 < n \le N-4 \\ \frac{2\pi(N-n)}{4} & N-3 \le n \le N. \end{cases}$
Square BPP	$a_n, b_n \sim U\left(-\frac{L}{2}, \frac{L}{2}\right)$	$p_U(u) = \begin{cases} \frac{1}{L} & -\frac{L}{2} \le u \le \frac{L}{2} \\ 0 & \text{otherwise.} \end{cases}$
Matern type II HCPP	$a_n, b_n \sim U\left(-\frac{L}{2}, \frac{L}{2}\right)$	$\lvert(a_p - a_q, b_p - b_q)\rvert > \delta,$ $\forall p, q \in \{1, \cdots, N\},$ $\mathbb{E}_\Phi[N] = \lambda_{mpp}.$

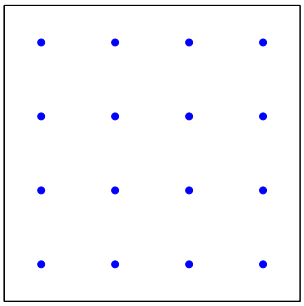

(a) Square array geometry

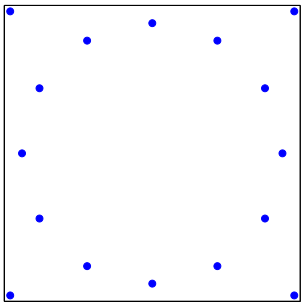

(b) Circle-square geometry

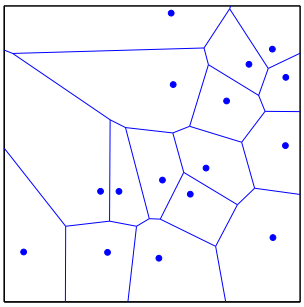

(c) Realization of BPP

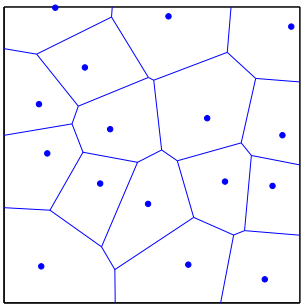

(d) Realization of HCPP

Fig. 2. LED deployment for various geometries.

2.1. *Generation of matern process of type II*

The HCPP in Fig. 2d resembles the possible distribution of LEDs at the source. In this point process, points are genreated from a stationary parent Poisson point process (PPP) of intensity λ_{ppp} and a random mark is associated with each point, and a point of the parent Poisson process

Optics EXPRESS

is deleted if there exists another point within the hard-core distance δ with a smaller mark. The intensity of the Matern point process is [23]

$$\lambda_{mpp} = \lambda_{ppp} e^{-\lambda_{ppp}\pi\delta^2} \tag{2}$$

2.2. Quality factor

The quality factor, defined in [13] for measuring the illuminance performance of the light source, can be expressed as

$$F_\Lambda = \frac{\overline{\Lambda}}{2\sqrt{\text{var}(\Lambda)}}, \tag{3}$$

where

$$\Lambda_j = \frac{P_{r_j}^2}{\sigma_j^2} \tag{4}$$

is the received *electrical* SNR at the jth photodetector and $\overline{\Lambda}$ and var(Λ) are the mean and variance of $\{\Lambda_j\}_{j=1}^K$, where K is the number of photodetectors. σ_j^2 is the noise variance explained in detail in [22]. For uniform illumination, it is important that the mean $\overline{\Lambda}$ be large and the variance var(Λ) be small, resulting in high quality factor (3). Since the output of the photodetector is an electrical signal which is affected by noise, it is important to consider the electrical SNR Λ_j while computing the quality factor in (3). Since the SNR at the receiver is proportional to square of received power (or received power) in low transmit power regime (or high transmit power), the power allocation for uniform illuminance also results in uniform SNR. In [24], SNR was expressed in terms of illuminance and shown to be proportional to illuminance.

For the uniform illuminance in VLC system, the power received at any photo detector on the receiver plane should be same. Since the photo detectors can be located at any point in the plane, the variance of the received power is considered as a objective function to be minimized

$$\min_{P_{t_i}} \quad \mathbb{E}\left[\left(P_{r_j} - \mathbb{E}\left[P_{r_j}\right]\right)^2\right] \tag{5}$$

This can be formulated as an optimization problem. The objective function in (5) is expressed in quadratic form as (See Appendix A)

$$\begin{aligned} \min_{x} \quad & \frac{1}{2}\mathbf{x}^T\mathcal{P}\mathbf{x} \\ \text{subject to} \quad & \mathcal{G}\mathbf{x} \preceq \mathbf{0} \\ & \mathcal{A}\mathbf{x} = P \end{aligned} \tag{6}$$

where $\mathcal{G} = \text{diag}(-1, \cdots, -1)$, $\mathcal{A} = [1, \cdots, 1]$ and elements β_{uv} of matrix $\mathcal{P}$ are given by

$$\beta_{uv} = \begin{cases} \frac{2\sum_{p=1}^K H_{up}^2}{K} - \frac{2\left(\sum_{p=1}^K H_{up}\right)^2}{K^2}, & u = v \\ \frac{2\sum_{p=1}^K H_{up}H_{vp}}{K} - \frac{2\left(\sum_{p=1}^K H_{up}\right)\left(\sum_{p=1}^K H_{vp}\right)}{K^2}, & u \neq v \end{cases} \tag{7}$$

The cost function in (6) is convex $\Leftrightarrow$ $\mathcal{P}$ is positive-definite [25]. Since the variance of received power $\mathbf{x}^T\mathcal{P}\mathbf{x} > 0 \quad \forall \quad \mathbf{x} \in \mathbb{R}_+^N$, $\mathcal{P}$ is positve-definite. Since the linear functions are both convex and concave, all the constraints are convex. Thus the optimization problem in (6) yields a quadratic and convex optimization problem. It can be numerically solved using quadratic programming (QP) through CVXOPT solver in Python .

Optics EXPRESS

Table 2. **Simulation Parameters**

Parameters	Symbol	Configuration
Room size	$L \times B \times D$	$5m \times 5m \times 3m$
Height of receiver plane	h_r	$0.85m$
LED semiangle	$\phi_{\frac{1}{2}}$	60^o

3. Results

All the physical parameters for the system have been obtained from [4] and Table 2.

The values of $\alpha = 1.1, 1.2, 3.1, 1.6$ of heuristic power allocation $\left(P_{t_i} = \frac{r_i^\alpha}{\sum_{j=1}^{N} r_j^\alpha} P\right)$ for Square, Circle-square, BPP and HCPP geometries respectively are obtained by golden section search algorithm. The variance and quality factor for different power allocation in different geometries have been tabulated in 3 and 4. It can be seen that the optimum solution obtained by solving (6) gives the minimum variance and better quality factor. The circle square geometry in [13] gives best quality factor, because of considering suboptimal location of LEDs. All results indicate that more the LEDs are distributed, more uniformity can be achieved with optimum power allocation.

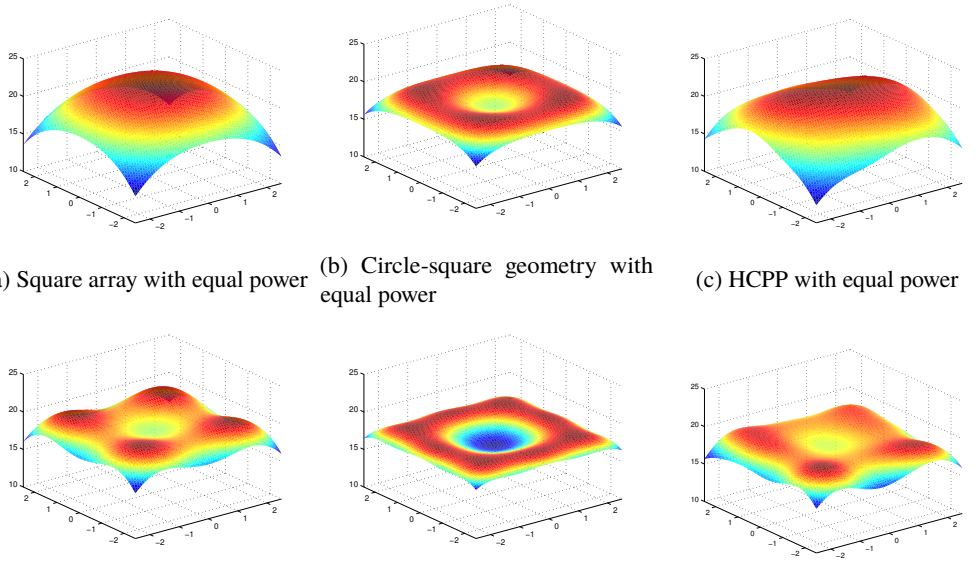

(a) Square array with equal power (b) Circle-square geometry with equal power (c) HCPP with equal power

(d) Square array with optimum power (e) Circle-square geometry with optimum power (f) HCPP with optimum power

Fig. 3. SNR profiles for different geometries.

In Fig. 3 the SNR profiles of different geometries for equal and optimum power allocation schemes are plotted. Note that SNR profile of HCPP is for one realization of the point process.

In Fig. 4 the optimal allocation of total transmit power $P = 2W$ across 16 source LEDs distributed according to HCPP is shown. It was observed that 3 source LEDs marked red in Fig. 4a have insignificant transmit power compared to others. Hence, these LEDs are taken out of geometry in Fig. 4b keeping others at the same location. The optimum power allocation for these 13 LEDs obtained once again through solvers still preserves uniform illuminance. This can be seen from Table 3 and 4, where the variance and the quality factor of the HCPP model

Optics EXPRESS

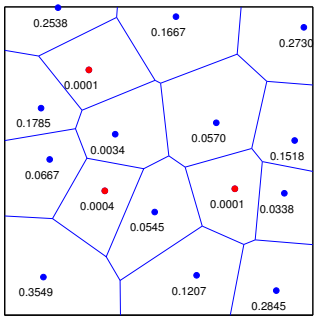

(a) HCPP with N=16 LEDs

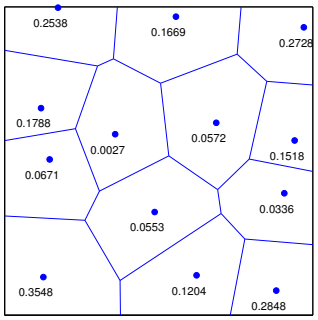

(b) HCPP with N=13 LEDs

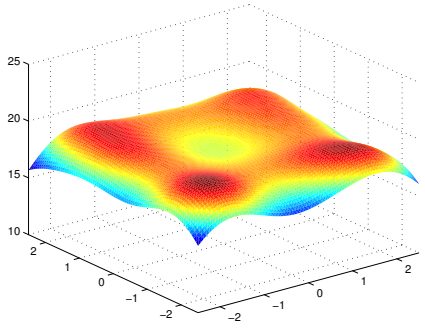

(c) SNR profile of 16 LED realization of HCPP

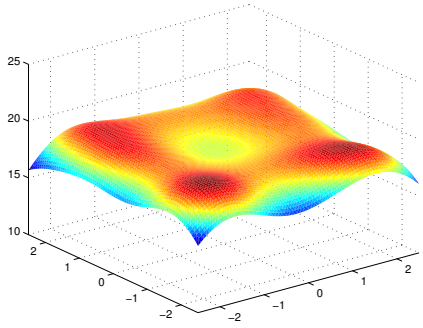

(d) SNR profile of 13 LED realization of HCPP

Fig. 4. Optimal distribution of total transmit power across source LEDs and their SNR profiles.

Table 3. **Variance of Received Power**

Geometry	**Equal Power**	**Heuristic [22]**	**Optimum**
Square Array	6.4414e-15	6.5287e-16	6.3785e-16
Circle Square	3.0134e-15	1.1267e-15	8.0382e-16
BPP	2.5589e-14	5.4944e-15	2.7167e-15
HCPP(16 *LEDs*)	6.9160e-13	1.9802e-13	3.3046e-14
HCPP(13 *LEDs*)	4.4503e-13	1.5460e-13	3.3027e-14

Table 4. **Quality Factor**

Geometry	**Equal Power**	**Heuristic [22]**	**Optimum**
Square Array	1.24	3.30	3.28
Circle Square	3.79	4.48	5.06
BPP	1.27	2.80	3.49
HCPP(16 *LEDs*)	1.16	1.92	4.26
HCPP(13 *LEDs*)	1.39	2.10	4.26

realization with 13 source LEDs is close to the realization with 16 LEDs, thus reducing the cost

Optics EXPRESS

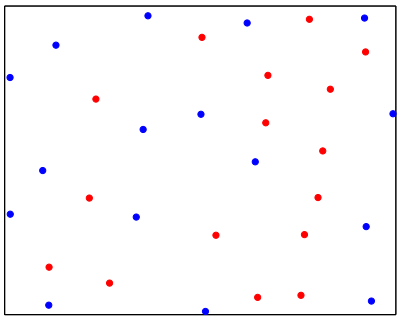

(a) HCPP with intensity λ_{mpp}=32 and threshold 0.0027

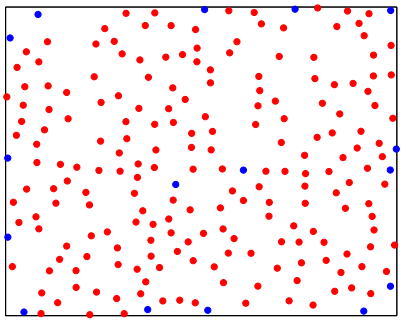

(b) HCPP with intensity λ_{mpp}=200 and threshold 0.017

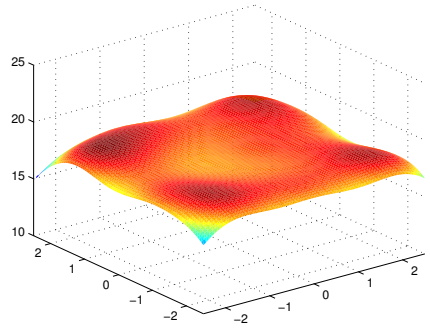

(c) SNR profile of the above realization with 16 LEDs resulting in quality factor F_Λ = 6.29

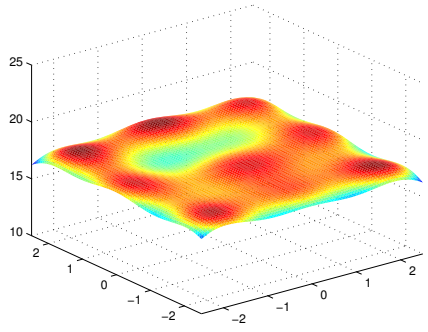

(d) SNR profile of the above realization with 16 LEDs resulting in quality factor F_Λ = 11.35

Fig. 5. Optimal distribution of total transmit power across source LEDs and their SNR profiles.

of the system.

In Fig. 5 the source LEDs are distributed according to HCPP with intensity of 32 and 200. The LEDs are taken out of geometry in Fig. 5a and Fig. 5b, in case the transmitted power is less than threshold. It is observed from Fig. 4a, Fig. 5a and Fig. 5b that the uniformity and the quality factor are improved for the same number of LEDs. This improvement can be attributed to optimum location of LEDs.

In Fig. 6 the quality factor and number of source LEDs are plotted with respect to the transmit power threshold. It can be seen that the quality factor saturates as the number of source LEDs increases. For a ideal VLC system, the high quality factor should be acheived with the less number of source LEDs. Hence, there is a tradeoff between the number of LEDs and the quality factor (Table 5). For example, at threshold value of 0.016 the quality factor is 14.02 and close to the saturated value. The number of LEDs required for obtaining that quality factor is 17. Thus, the performance curves in Fig. 6 can be used to estimate the cost of the VLC system in terms of the number of LEDs.

Optics EXPRESS

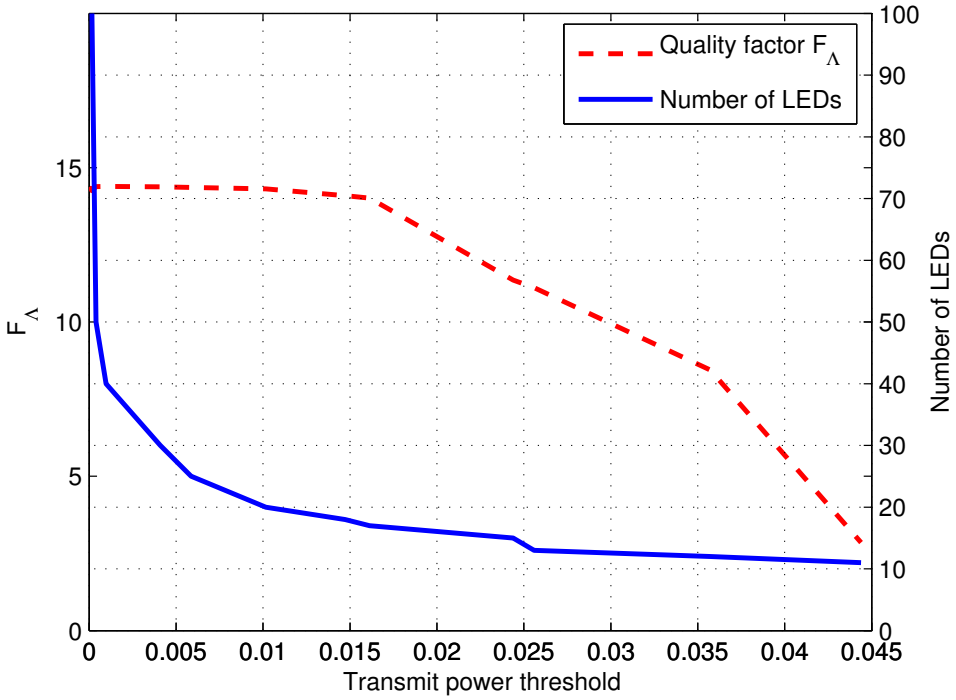

Fig. 6. Performance of HCPP model with intesity λ_{mpp} = 200.

Table 5. **Quality Factor**

Intensity of HCPP	**Transmit power threshold**	**Number of LEDs remaining for realization**	**Quality factor**
16	0	16	4.26
32	2.7e-3	16	6.29
200	1.7e-2	16	11.34
	1.6e-2	17	14.02

4. Conclusion

This paper considered the optimization of power allocation to source LEDs for uniform illumination in VLC. The problem was formulated as a quadratic optimization problem and resolved numerically using CVXOPT solver. Numerical results demonstrate that the uniform illumination can be acheived even when all light sources are distributed randomly, in contrast with the existing fixed geometries like circular and square arrays. It was observed that HCPP model can preserve uniformity with less number of LEDs compared to other geometries, thus reducing the cost of the system. It would be useful to compare the BER performance for various geometries considered in the paper. This will be the focus of future work.

Optics EXPRESS

A. Formulation of optimization problem

A.1. Cost function

The first term in (5) is expressed in terms of transmit power as

$$\begin{aligned}\mathbb{E}\left[\left(P_{r_j}\right)^2\right] &= \mathbb{E}\left[\left(\sum_{i=1}^{N} H_{ij}P_{t_i}\right)^2\right] \qquad \text{(From (1))}\\ &= \mathbb{E}\left[\sum_{i=1}^{N} H_{ij}^2 P_{t_i}^2 + 2\sum_{i=1}^{N}\sum_{q=i+1}^{N} H_{ij}H_{qj}P_{t_i}P_{t_q}\right]\\ &= \frac{\sum_{j=1}^{K}\sum_{i=1}^{N} H_{ij}^2 P_{t_i}^2}{K} + \frac{\sum_{j=1}^{K} 2\sum_{i=1}^{N}\sum_{q=i+1}^{N} H_{ij}H_{qj}P_{t_i}P_{t_q}}{K}\\ &= \frac{\sum_{i=1}^{N}\mu_{ii}P_{t_i}^2 + 2\sum_{i=1}^{N}\sum_{q=i+1}^{N}\mu_{iq}P_{t_i}P_{t_q}}{K} \qquad (8)\\ &\text{where } \mu_{iq} = \sum_{j=1}^{K} H_{ij}H_{qj}.\end{aligned}$$

Similarly, the second term is expressed as

$$\begin{aligned}\left(\mathbb{E}\left[P_{r_j}\right]\right)^2 &= \left(\frac{\sum_{j=1}^{K} P_{r_j}}{K}\right)^2 = \left(\frac{\sum_{j=1}^{K}\sum_{i=1}^{N} H_{ij}P_{t_i}}{K}\right)^2 \qquad (9)\\ &= \left(\frac{\sum_{i=1}^{N}\gamma_i P_{t_i}}{K}\right)^2 \text{ where } \gamma_i = \sum_{j=1}^{K} H_{ij}\\ &= \frac{\sum_{i=1}^{N}\gamma_i^2 P_{t_i}^2 + 2\sum_{i=1}^{N}\sum_{p=i+1}^{N}\gamma_i\gamma_p P_{t_i}P_{t_p}}{K^2}. \qquad (10)\end{aligned}$$

Using (9) and (8) in (5), variance is represented in matrix form as

$$\begin{aligned}\text{var}\left(P_{r_j}\right) &= \frac{\sum_{i=1}^{N}\mu_{ii}P_{t_i}^2 + 2\sum_{i=1}^{N}\sum_{q=i+1}^{N}\mu_{iq}P_{t_i}P_{t_q}}{K} - \frac{\sum_{i=1}^{N}\gamma_i^2 P_{t_i}^2 + 2\sum_{i=1}^{N}\sum_{p=i+1}^{N}\gamma_i\gamma_p P_{t_i}P_{t_p}}{K^2}\\ &= \sum_{i=1}^{N}\frac{\mu_{ii}}{K} - \frac{\gamma_i^2}{K^2}P_{t_i}^2 + 2\sum_{i=1}^{N}\sum_{q=i+1}^{N}\frac{\mu_{iq}}{K} - \frac{\gamma_i\gamma_p}{K^2}P_{t_i}P_{t_q}\\ &= \frac{1}{2}\sum_{i=1}^{N}\left(\frac{2\sum_{j=1}^{K}H_{ij}^2}{K} - \frac{2\left(\sum_{j=1}^{K}H_{ij}\right)^2}{K^2}\right)P_{t_i}^2\\ &\quad + 2\sum_{u=1}^{N}\sum_{v=i+1}^{N}\left(\frac{2\sum_{j=1}^{K}H_{uj}H_{vj}}{K} - \frac{2\left(\sum_{j=1}^{K}H_{uj}\right)\left(\sum_{j=1}^{K}H_{vj}\right)}{K^2}\right)P_{t_u}P_{t_v}\\ &= \frac{1}{2}\left[P_{t_1},\cdots,P_{t_N}\right]\begin{bmatrix}\beta_{11} & \cdots & \beta_{1N}\\ \vdots & \ddots & \vdots\\ \beta_{N1} & \cdots & \beta_{NN}\end{bmatrix}\begin{bmatrix}P_{t_1}\\ \vdots\\ P_{t_N}\end{bmatrix}\\ &= \frac{1}{2}\mathbf{x}^T\mathcal{P}\mathbf{x}. \qquad (11)\end{aligned}$$

Optics EXPRESS

A.2. Constraints

1. The total power of the LEDs is P watts, which is distributed across the source LEDs.

$$\sum_{i=1}^{N} P_{t_i} = P$$
$$\Rightarrow \mathcal{A}\mathbf{x} = P$$

where $\mathcal{A} = [1, \cdots, 1]$.

2. The power of each source LED is always non-negative.

$$-P_{t_i} \leq 0 \forall i \in 1, \cdots, N$$

which can be expressed in matrix form as

$$\Rightarrow \mathcal{G}\mathbf{x} \preceq \mathbf{0}$$

where $\mathcal{G} = \text{diag}(-1, \cdots, -1)$.